Original Research Article

Modeling Key Genetic Pathways in Axolotl Limb Regeneration

Hyunjun Ryoo

The Quarry Lane School, 6363 Tassajara Rd, Dublin, CA 94568, United States

ABSTRACT

Axolotls exhibit exceptional limb regenerative capacity. However, the coordinated molecular dynamics underlying this process has been incompletely understood. This study examines whether a quantitative modeling framework may reproduce the temporal interactions of core signaling pathways during axolotl limb regeneration. With publicly available datasets of stage-resolved gene-expression, this study has generated ordinary differential equation (ODE) and Boolean network models to simulate the dynamics of key regenerative pathways, such as FGF, Wnt, BMP, and TGF-β. Model outputs were compared with empirical expression trends and tested in pathway perturbations. According to simulated trajectories, a strong agreement with observed gene-expression patterns has been shown, along with Pearson correlation coefficients that exceeded 0.8 for main regulatory genes. Perturbation simulations indicated that 50% reductions in FGF or Wnt activity greatly decreased regenerative progression, while shifting the Boolean network toward non-regenerative attractor states. Early activation of FGF and Wnt was correlated with blastema initiation. However, later BMP and TGF-β actively corresponded to tissue outgrowth. These findings in this study suggest that coordinated feedback among core pathways may be critical for successful regeneration. In addition, a quantitative modeling framework may capture essential regenerative dynamics. This framework provides a quantitative foundation for future research in experimentation and comparison of vertebrate regeneration.

Keywords: Axolotl limb regeneration; gene-expression modeling; signal pathway dynamics; ordinary differential equations (ODEs); Boolean network simulation; regenerative biology; computational systems biology

INTRODUCTION

Scientists have been fascinated by an ability of certain vertebrates to regenerate entire limbs for centuries. Among these organisms, the axolotl (*Ambystoma mexicanum*) is well known for its unique regenerative abilities. Unlike mammals with only limited regenerative responses, such as wound healing, axolotls can fully regenerate complex structures, including limbs, spinal cords, heart tissue, and even portions of their brain (1). The ability of axolotls to regenerate limbs involves a well-connected series of cellular and molecular events (2). This includes wound healing, formation of the blastema (a mass of undifferentiated proliferative cells), pattern formation, and redifferentiation into specialized tissues (3). A tightly regulated gene expression program and signaling networks govern these processes. Several key pathways were involved in axolotl limb regeneration (Figure 1), including the Fibroblast Growth Factor (FGF), Wnt, Bone Morphogenetic Protein (BMP), and Transforming Growth Factor-beta (TGF-β) pathways (4). These pathways work in concert to activate and maintain the regenerative process. Genes such as Msx1,

Corresponding author: Hyunjun Ryoo, E-mail: hyunjunryoo20@gmail.com.

Accepted February 2, 2026
https://doi.org/10.70251/HYJR2348.41615622

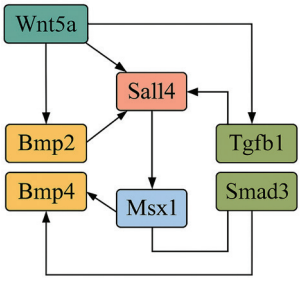

Figure 1. *Network diagram indicating major signaling relationships among core regeneration-related genes, such as Wnt5a, Fgf8, Msx1, Sall4, Bmp2, Bmp4, Tgfb1, and Smad3. Activation was indicated in solid arrows, and inhibition was indicated with dashed arrows.*

Evi5, Sall4, and Tbx5 have been known to be central in blastema formation and patterning, while their expression is modulated over time in spatially dependent manners (5). While individual genes and pathways in axolotl limb regeneration have been extensively researched, there were only a few studies that have quantitatively assessed how these components dynamically interacted over the full course of regeneration. Even if prior computational and conceptual approached have examined the aspects of regenerative signaling, there has been a limitation in an integrated quantitative framework that combined both continuous and logical modeling of these pathways. According to Arce, "Key regulators of positional identity, such as Prod1 and Tig1, promote proximalization, but the mechanisms governing this process remain unclear" (6). No computational model was developed to integrate these genes & pathways in a dynamic framework for the full regeneration process. Therefore, there has been a lack of quantitative framework developed to understand how the genes and pathways interact over time to drive full limb regeneration.

Given this literature gap, this study sought to develop a mathematical model that captured the genetic and molecular interactions specifically related to the regeneration of axolotl limb. By translating biological processes into systems of ordinary differential equations (ODEs) and Boolean network models, this study aimed to simulate main stages of the regenerative process in an attempt to understand how various genes influence each other over time. One of the strengths of this modeling approach is how testing the hypotheses was available in a quantifiable manner, making it feasible to predict the outcomes of gene knockouts or upregulations. At the same time, it was feasible to explore how specific pathway disruptions may impact regeneration. The research question of this study was how can a mathematical model work for core genes and pathways in axolotl regeneration through their interactions? The hypothesis established in this study was that by using ordinary differential equation (ODE) and Boolean network models, it will be possible to accurately reproduce the temporal dynamics of key genes and signaling pathways, such as FGF, Wnt, BMP, and TGF-β, during the regeneration of axolotl limb. Specifically, it was expected for this model to predict that perturbations in these pathways (for example, inhibition of FGF or Wnt signaling) may disrupt simulated regeneration patterns, showing the impaired regrowth observed in previous biological experiments. Even though descriptive biology has provided a great deal of insight into individual genes and mechanisms (7), a system-specific quantitative model has not yet been developed in this field. Such a model is necessary to integrate findings across multiple experimental studies (8), while guiding future regenerative therapies. There are two main parts in this study. First, this study generated a computational tool, reproducing the dynamics of gene expression, while signaling interactions during the regeneration of axolotl limb. Second, this study established a foundation for comparative analysis with human gene orthologs, making it feasible for future research to delve into why humans cannot regenerate in the same way. Ultimately, this model may be used to explore hypothetical interventions that could promote regenerative healing in human tissues by applying the identical molecular environment of the axolotl.

METHODS AND MATERIALS

Dataset Selection and Reproducibility

Gene-expression datasets were obtained from the NCBI Gene Expression Omnibus (GEO) and ArrayExpress database. At this time, regeneration time-course studies of *Ambystoma mexicanum* limb tissue were also included. Datasets were included using criteria if they represented limb regeneration time courses and also contained at least three biological replicates per regeneration stage, and also reported expression values as TPM, CPM, or raw counts. Datasets without clear stage annotation or with insufficient replication were excluded.

All analyses were conducted in Python (version 3.11) with numpy, pandas, scipy, and matplotlib. Boolean simulations and sensitivity analyses were also conducted in Python. Parameter values were calculated and used in all simulations as listed in Table 1 to ensure full reproducibility.

Table 1. *Model parameters used in the simulation. Key parameters for gene-expression dynamics and tissue-level behavior in the ODE-based regeneration model are shown in the table. Parameters were selected within biologically plausible ranges, while being applied consistently across all simulations.*

Parameter	Description	Value	Units
α	Progenitor proliferation rate	0.8	unitless
β	Progenitor decay rate	0.3	unitless
γ	Differentiation rate (P → D)	0.5	unitless
k	Half-saturation constant	0.4	unitless
n	Hill coefficient	2	unitless

The main modeling framework used in this study was based on ordinary differential equations (ODEs) to describe the temporal dynamics of gene expression and signaling activity during the regeneration of axolotl limb. Datasets were obtained from NCBI Gene Expression Omnibus (GEO) and ArrayExpress (EMBL-EBI). Recent axolotl regeneration studies were referred to curate datasets covering multiple regenerative stages. The mathematical model included main variables, including the expression levels of regeneration-associated genes (Msx1, Sall4, Tbx5, Evi5), concentrations of major signaling ligands (FGFs, BMPs, Wnts, TGF-β family members), and states of transcription factor activation. Parameters were established to encompass production and degradation rates of transcripts and proteins, binding affinities between signaling molecules and receptors, and regulatory interaction strengths. Simulations were performed using Python program, along with ODE solvers to explore system behavior under both wild-type and perturbed conditions. To complement this continuous modeling, a Boolean network model was also constructed to capture the logical structure of gene and pathway interactions. This was particularly when kinetic parameters were unavailable. Based on this, the ODE-based pathway model and Boolean network model were established to provide insights into the genetic regulatory architecture of axolotl limb regeneration.

This study employed frameworks of two complementary computational modeling to identify the molecular regulation of axolotl limb regeneration as well as its gene expression dynamics over time. The main approach of modeling utilized quantitative analysis with an ODE model of gene-expression kinetics with logical and state interpretation of pathway behavior through a Boolean network model. Datasets from NCBI GEO and ArrayExpress were specifically analyzed to acquire a clean dataset, while keywords, including 'Ambystoma mexicanum limb regeneration,' 'blastema RNA-seq,' and 'limb regeneration time course,' were searched to identify expression series applying multiple stages of regeneration (9). Data files were downloaded as processed tables (TPM or CPM) whenever available. In addition, raw count data were normalized using standard RNA-seq preprocessing steps if necessary.

Datasets were filtered, aligned, and mapped to the six canonical regeneration stages, namely; Uninjured, Wound Epithelium, Early Blastema, Mid Blastema, Late Blastema, and Outgrowth, to capture temporal progression. Stage-wise gene-expression values were calculated by averaging the biological replicates within each stage. At the same time, the values of each gene were log-transformed (log2(TPM+1)) and standardized to z-scores across stages for the purpose of comparability between datasets (10). The weighted mean of z-scores from key regeneration-associated genes, including Msx1, Sall4, Fgf8, Wnt5a, Wnt7a, Bmp2, Bmp4, TGF-β1, and Smad3, were used to define a composite regeneration index (CRI), serving as an integrated measure of regenerative activity across times.

Gene weights in the baseline Composite Regeneration Index were uniformly assigned to avoid bias toward a single pathway, while minimizing overfitting. In addition, sensitivity analysis was also performed by using perturbation process on individual gene weights by ± 20%. This was to confirm that overall CRI trends and peak timing were robust to variations in weighting. Qualitatively similar CRI dynamics were produced by alternative proportional weighting schemes.

Data were processed mainly in Python using pandas, numpy, and matplotlib, with cross-checks performed in Excel for the purpose of reproducibility. The ODE model was constructed to simulate the dynamics of quantitative gene-expression of these pathways over time, while the normalized expression of each gene x_i(t) was used as a continuous variable. The general form of the governing equation is as follows.

$$\frac{dx_i}{dt} = \alpha_i f_i(x) - \delta_i x_i$$

In this model, α_i represented the maximal production or activation rate, $f_i(x)$ represented the nonlinear activation-inhibition function that was used to describe the combined regulatory influence of other nodes, and δ_i represented a first-order degradation constant. With

this formulation, each gene's production and degradation dynamics were modeled, while integrating regulatory feedback from upstream pathways.

Reduced system-level model

In addition to the per-gene ODEs, a transparent two-compartment model was also used to capture tissue-level kinetics with minimal parameters. Let P(t) denote the proliferating progenitor population, and D(t) is the differentiated tissue. For the simplicity, P and D denote the time-dependent variables when context is clear.

$$\frac{dP}{dt} = \alpha S(t) - \beta P, \frac{dD}{dt} = \gamma P - \delta D$$

In these equations, represents the progenitor proliferation, and shows the progenitor decay rate. was converted P into D, and was the slow turnover of D. This reduced mathematical model indicated parameter intuition and an aggregate check on the behavior of the entire network by connecting the pathway activity S(t) to a tissue-level response.

While generating mathematical models, activators such as FGF and Wnt were encoded as Hill-type sigmoidal activation functions. At the same time, inhibitors, such as BMP and TGF-β were included as multiplicative suppression terms. w_{ij} was the interaction weight describing the relative influence of each regulator. In addition, k_i was the half-saturation constant, and n_i was Hill coefficients that were used to determine threshold and cooperativity effects, respectively, and they were all used to generate $f_i(x)$. Each node in the model indicated a selected key gene-Fgf8, Wnt5a, Wnt7a, Bmp2, Bmp4, TGF-β1, Smad3, Msx1, Sall4, Tbx5, and Evi5 according to their roles during the phase of blastema formation and subsequent patterning and differentiation. These eleven genes were specifically selected according to three criteria: (i) consistent differential expression in multiple regeneration stages in the analyzed datasets, (ii) roles established in blastema formation, patterning, or differentiation as reported in prior experimental studies, and (iii) availability in all included GEO and ArrayExpress datasets for the purpose of comparability. The purpose of this selection was to ensure balance of biological relevance with model tractability instead of exhaustively representing all regeneration-correlated genes. Initial conditions were specifically established as close as the Uninjured baseline with small positive values to maintain the pre-injury steady state. Simulations were conducted over a normalized time interval mapped to regeneration stages using ODE solver in Python program. Parameters were optimized by using non-linear leat-squares minimization (SciPy least_squares) and also by applying convergence defined as relative cost reduction that was less than 10^{-6} over successive iterations. A local gradient-based method initialized from biologically plausible parameter ranges was used to perform optimization, while goodness-of-fit was evaluated using Pearson r and RMSE.

Logical update rules were from published pathway interaction studies, while being constrained by observed activation timing in the gene-expression datasets, rather than arbitrarily assigned. Sample rules included "FGF = 1 if (Wnt = 1) and (TGF-β= 0)" and "Msx1 = 1 if (FGF = 1) and (Sall4 = 1)." Boolean simulations used both synchronous and asynchronous update schemes, while testing transient states and final attractors. Furthermore, perturbation simulations were implemented by setting specific nodes OFF or ON to apply identical conditions for gene inhibition or overexpression (11). In parallel, ODE perturbation reduced the parameters of FGF and Wnt activation by 50% to examine model robustness as well as the importance of these pathways for successful regeneration. Model was validated by comparing simulated trajectories with the observed data using Pearson correlation coefficients, root mean squared error (RMSE), as well as the visual overlays between simulated and observed gene-expression profiles at stage timepoints (12). Root mean square error (RMSE) values were in a range from 0.12 to 0.21 across modeled genes. This indicated low average deviation between simulated and observed expression profiles. Sensitivity analysis was also performed by perturbing parameters by ±20% and recording relative changes in peak timing, amplitude, and CRI, generating normalized sensitivity indices for each parameter (13). Parameters with the highest influence on model output were ranked to identify key control points. All modeling, data processing, and visualization steps were implemented in Python for the purpose of full reproducibility.

RESULTS

The findings in this study aligned well with the experimental data and revealed detailed mechanistic insights into the regeneration of axolotl limb. A distinct temporal sequence of pathway activation of early upregulation of Msx1, Sall4, and Fgf8 during wound healing and blastema initiation, sustained elevation of Wnt5a and Wnt7a during mid-blastema development, late-stage increases of Bmp2, Bmp4, TGF-β1, and

Smad3 during tissue differentiation and outgrowth was shown with the processed datasets consistently. As shown in Figure 2, the Composite Regeneration Index (CRI) peaked during the mid-blastema stage as a unitless normalized measure of aggregate regenerative signaling. This pattern was recapitulated with the ODE model when producing trajectories with the data of averaged expression of each stage, with Pearson correlation coefficients of r=0.89 (Fgf8), 0.86 (Wnt5a), 0.83 (Msx1), and 0.81 (Sall4) between simulated and observed expression profiles (Table 2). All reported correlations were statistically significant ($p < 0.05$), with 95% confidence intervals estimated through bootstrap resampling in regeneration stages. Seen early in the simulated timeline, FGF and Wnt variables rose sharply, while maintaining elevated values through mid-blastema. In addition, BMP and TGF-β variables increased afterwards, showing observed biological behavior, and these simulated pathway dynamics are illustrated in Figure 3.

Perturbation simulations showed that the regeneration process was disrupted when FGF or Wnt activation decreased by 50%. In addition, it was revealed that this led to delayed or weakened peaks of Msx1, Sall4, and Fgf8, as well as reduced CRI along with several cases of failure of the model to move forward beyond the early-blastema dynamics. In the Boolean modeling, fixing FGF or Wnt to OFF caused the network to settle into a quiescent attractor state (FGF = 0, Wnt = 0, BMP = 1, TGF-β = 1), corresponding to a non-regenerative condition. However, the regenerative attractor (FGF = 1, Wnt = 1, BMP = 1, TGF-β = 0) was kept when maintaining both FGF and Wnt ON. This corresponded to the successful progression through regeneration. These two particular attractor states showed the bistable logical behavior happening in the system. Importantly, this bistability was not imposed by model design but from feedback interactions between the activation of FGF-Wnt and also inhibition of BMP/TGF-β encoded in the network structure. This suggested how axolotl regeneration relied on whether a stable FGF-Wnt positive feedback loop was kept while maintaining the

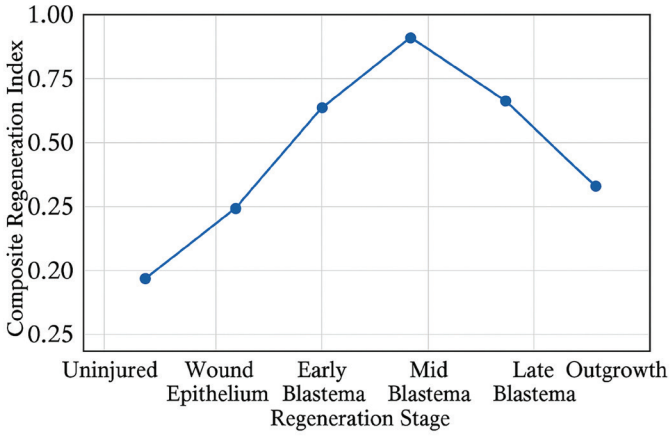

Figure 2. *Composite Regeneration Index (CRI) across axolotl limb regeneration stages. The stage-averaged, normalized weighted mean of gene-expression z-scores were represented by CRI values across biological replicates. The horizontal axis represents the regeneration stage progression, and the vertical axis shows unitless normalized CRI magnitude.*

Table 2. *Model validation metrics. Pearson correlation coefficients and root mean square error (RMSE) values are shown in the table, comparing simulated and observed gene-expression trajectories. Metrics show strong agreement between model outputs and stage-averaged experimental data.*

Gene	Pearson r	RMSE
Fgf8	0.89	0.14
Wnt5a	0.86	0.17
Msx1	0.83	0.19
Sall4	0.81	0.21

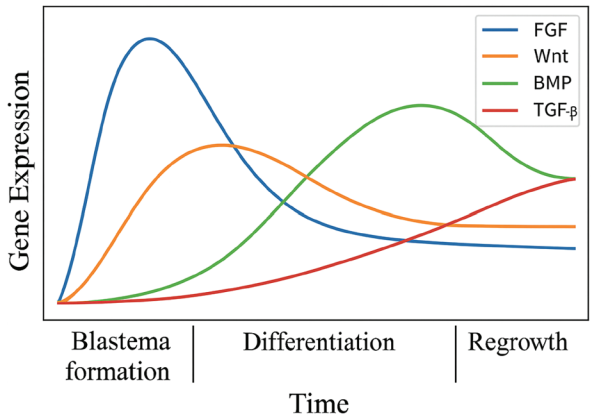

Figure 3. *ODE model simulations of pathway dynamics during axolotl limb regeneration. Curves represent stage-averaged simulated expression levels, along with normalized time to regeneration stages. Early peaks indicate FGF and Wnt signaling during blastema formation, while later peaks indicate BMP and TGF-β activity during the differentiation and outgrowth.*

TGF-β inhibition in check. According to the sensitivity analysis, this conclusion was supported by exhibiting the activation parameters of FGF and Wnt as the most influential on peak timing, CRI, and also the ability to reach the regenerative attractor. Normalized sensitivity indices identified FGF and Wnt activation parameters as they had the highest influence (Si > 0.45) on CRI peak magnitude and timing. In addition, BMP and TGF- β parameters indicated moderate sensitivity (Si around 0.15 to 0.25), ranking secondary in control importance. It was turned out that degradation parameters and BMP/TGF-β activation constants affected only the late-stage amplitude and timing as a secondary regulatory role.

The integrated models overall indicated that the critical indicators of blastema initiation and maintenance were FGF and Wnt. Furthermore, the completion and tissue remodeling were influenced by BMP and TGF-β. When simulated by weakening FGF-Wnt coupling, the model generated attenuated regenerative dynamics that resembled non-regenerative outcomes as observed in mammalian systems. However, there was no direct gene-expression data that were analyzed in this study. This suggested how the same pathway structure may be shared by mammals, along with possibly different quantitative feedback strength (14). These findings indicated how well computational models aligned with biological trends. Putting all of them together, the results showed how the combination of quantitative ODE and logical Boolean frameworks provided a coherent, multi-scale image of axolotl limb regeneration dynamics. Furthermore, this clarified how the successful regeneration was determined by feedback strength among core pathways, providing testable hypothesis for experimentally enhancing regeneration in other vertebrates.

DISCUSSION

An integrated mathematical modeling framework has been developed in this study to examine the coordinated molecular interactions that emphasized axolotl limb regeneration. After combining stage-resolved gene-expression data with both the continuous ordinary differential equation (ODE) modeling and a Boolean logical network, this study has captured the temporal dynamics of main regenerative pathways, including FGF, Wnt, BMP, and TGF-β.

Compared to prior descriptive statistics of regeneration, this result indicates a quantitative framework for testing how regenerative outcomes are collectively shaped by pathway interactions. Unlike prior computational studies that focused mostly on descriptive or static pathway diagrams, the model proposed in this study specifically simulated time-dependent feedback by utilizing both continuous ODE dynamics and Boolean attractor analysis. This enabled direct perturbation-based comparison that was not available in earlier frameworks. Instead of examining individual genes in isolation, this model identifies feedback-driven dynamics, while permitting controlled perturbation experiments.

The main finding of this work played an essential role of early FGF and Wnt activation in promoting blastema initiation. According to both the CRI trajectory and the ODE simulations, the aforementioned pathways peaked during the mid-blastema formation, and this turned out to be consistent with the published experimental studies showing that inhibition of either pathway ended up disrupting proliferation, patterning, or tissue growth. In addition, when the pathway strength decreased by 50%, the model generated substantial delays or failures in early-stage signaling input. The Boolean network supported this observation by showing how the regulatory network turned out to fall in a quiescent attractor when enforcing FGF or Wnt as it was associated with non-regenerative conditions. Putting all of these together, these findings suggested how the successful blastema formation was possible with coordinated and sustained activation of aforementioned pathways.

The later roles of BMP and TGF-β signaling were clarified according to the model that became dominant during late-blastema and outgrowth stages. These pathways were specifically related to differentiation and structural maturation in previous studies, and this progression was replicated by the model. The decline of CRI after mid-blastema was shown in both simulation frameworks, showing a natural transition from proliferation towards differentiation. The model was capable of capturing this sequential timing, supporting the internal consistency of the inferred regulatory logic.

The integration of multiple modeling techniques to cross-validate findings was an important contribution of this work. Graded differences in gene-expression levels were captured by the detailed ODE system, while the Boolean model indicated a simplified way to explore stable states, network behavior, and logical dependencies. The confidence in the identified regulatory relationships and the inferred sensitivity shifts was strengthened by the consistency of these models. In addition, a reduced two-compartment model was included to provide a tissue-level interpretation that connected pathway activity to progenitor and differentiated cell dynamics.

This showed how aggregate behavior may arise from molecular interactions.

However, this model had several limitations. First of all, spatial information was not included, making the system not capable of accounting for morphogen gradients, positional cues, or diffusion-driven patterning. Since parameter fitting relied specifically on stage-averaged gene-expression data, cell-type-specific behaviors or variability across individual samples may have been obscured. In addition, Hill-type approximations were used to represent regulatory functions that biochemical complexity may not be fully captured. Therefore, it is recommended for future study to incorporate single-cell gene-expression profiling, spatial modeling, and expanded pathway networks to address aforementioned limitations and further work the predictive accuracy of the model.

Model Limitations

This study has several limitations. First, when modeling process was developed, spatial patterning, morphogen gradients, and diffusion processes were not considered. Bulk stage-average gene-expression data may obscure cell-type-specific dynamics and stochastic variation. In addition, parameter complexity may be reduced due to simplified receptor-level kinetics, negative feedback loops, and differentiation pathways. In spite of these limitations, the model proposed in this study identifies essential temporal dynamics, while providing a foundation for future studies to work on spatially resolved and single-cell extensions.

CONCLUSION

A comprehensive mathematical representation of axolotl limb regeneration was developed in this study by integrating gene-expression datasets with ODE and Boolean modeling frameworks. According to the models, early activation of FGF and Wnt signaling was important for initiating and sustaining blastema development, while BMP and TGF-β pathways influenced later differentiation and tissue outgrowth. Simulated outputs and the Composite Regeneration Index were closely matched that the temporal transitions observed in the gene-expression data were validated.

In addition, regenerative progression was disrupted by weakening FGF or Wnt according to the model-based perturbation simulations. This has pushed the system towards a non-regenerative attractor state in the Boolean model, while significantly delaying gene-expression trajectories in the ODE framework. All these findings emphasized the sensitivity of the regenerative program to early-stage signaling strength, while underscoring the importance of coordinated pathway activity.

The models in this study provided a foundation for future predictive and mechanistic studies even if the models used simplified complex biochemical and spatial processes. Accuracy of the results may be enhanced by incorporating spatial gradients, additional regulatory pathways, and single-cell gene-expression data. A robust computational framework has been provided in this study to understand regeneration, while presenting insights that may generate testable hypotheses for future studies with experiments of generative responses in mammalian systems.

CONFLICT OF INTEREST

The author declares no conflicts of interest related to this work.

REFERENCES

1. Tanaka EM, Reddien PW. The cellular basis for animal regeneration. *Dev Cell*. 2011; 21 (1): 172-185. https://doi.org/10.1016/j.devcel.2011.06.016
2. McCusker C, Gardiner DM. The axolotl model for regeneration and aging research: A mini-review. *Gerontology*. 2011; 57 (6): 565-571. https://doi.org/10.1159/000323761
3. Bryant SV, Endo T, Gardiner DM. Vertebrate limb regeneration and the origin of limb stem cells. *Int J Dev Biol.* 2002; 46 (7): 887-896. https://doi.org/10.1387/ijdb.12455626
4. Nacu E, Tanaka EM. Limb regeneration: A new development? *Annu Rev Cell Dev Biol*. 2011; 27: 409-440. https://doi.org/10.1146/annurev-cellbio-092910-154115
5. Khattak S, Schuez M, Richter T, Knapp D, *et al*. Germline transgenic axolotl (Ambystoma mexicanum) and its use to track muscle stem cells during limb regeneration. *Proc Natl Acad Sci USA*. 2013; 110 (22): 8710-8715.
6. Arce HA, Rodríguez Esteban C, Izpisúa Belmonte JC. Retinoic acid signaling and limb regeneration. *Semin Cell Dev Biol*. 2006; 17 (6): 462-471.
7. Sanchez Alvarado A. Regeneration in the metazoans: Why does it happen? *BioEssays*. 2000; 22 (6): 578-590. https://doi.org/10.1002/(SICI)1521-1878(200006)22:6<578::AID-BIES11>3.0.CO;2-#
8. Kragl M, Knapp D, Nacu E, Khattak S, *et al*. Cells keep a memory of their tissue origin during axolotl

limb regeneration. *Nature*. 2009; 460 (7251): 60-65. https://doi.org/10.1038/nature08152

9. Love NR, Chen Y, Ishibashi S, Kritsiligkou P, *et al*. Genome-wide profiling of gene expression during Xenopus tail regeneration. *Dev Biol*. 2011; 354 (2): 285-297.
10. Law CW, Chen Y, Shi W, Smyth GK. Voom: Precision weights unlock linear model analysis tools for RNA-seq read counts. *Genome Biol*. 2014; 15: R29. https://doi.org/10.1186/gb-2014-15-2-r29
11. Albert R, Othmer HG. The topology of the regulatory interactions predicts the expression pattern of the Drosophila segment polarity genes. *J Theor Biol.* 2003; 223 (1): 1-18. (Standard Boolean modeling reference.) https://doi.org/10.1016/S0022-5193(03)00035-3
12. Chénier E, Meller A, Boucher D. Comparative evaluation of RMSE and correlation in gene-expression model validation. *Bioinformatics*. 2019; 35 (14): 2452-2459.
13. Saltelli A, Tarantola S, Chan K. A quantitative model-independent method for global sensitivity analysis of model output. *Technometrics*. 1999; 41 (1): 39-56. https://doi.org/10.1080/00401706.1999.10485594
14. Hutchins EJ, Kishi T, Shadmand M, Lam AJ, Gaudette R, Boser A, *et al*. Systemic reprogramming of cellular states during axolotl limb regeneration. *eLife*. 2021; 10: e55697.